Development/Plasticity/Repair

Opposing Extracellular Signal-Regulated Kinase and Akt Pathways Control Schwann Cell Myelination

Toru Ogata,[1] **Satoru Iijima,**[1,2] **Shinya Hoshikawa,**[1] **Toshiki Miura,**[1] **Shin-ichi Yamamoto,**[1] **Hiromi Oda,**[1]
Kozo Nakamura,[1] **and Sakae Tanaka**[1]

[1]Department of Orthopaedic Surgery, Faculty of Medicine, The University of Tokyo, 7-3-1 Hongo, Bunkyo-ku, Tokyo 113-0033, Japan, and [2]Department of Orthopaedic Surgery, Juntendo University School of Medicine, 2-1-1 Hongo, Bunkyo-ku, Tokyo 113-8421, Japan

Schwann cells are the myelinating glia of the peripheral nervous system, and their development is regulated by various growth factors, such as neuregulin, platelet-derived growth factor (PDGF), and insulin-like growth factor-I (IGF-I). However, the mechanism of intracellular signaling pathways following these ligand stimuli in Schwann cell differentiation remains elusive. Here, we demonstrate that in cultured Schwann cells, neuregulin and PDGF suppressed the expression of myelin-associated protein markers, whereas IGF-I promoted it. Although these ligands activated common downstream signaling pathways [i.e., extracellular signal-regulated kinase (Erk) and phosphatidylinositol-3-kinase (PI3K)–Akt pathways], the profiles of activation varied among ligands. To elucidate the function of these pathways and the mechanisms underlying Schwann cell differentiation, we used adenoviral vectors to selectively activate or inactivate these pathways. We found that the selective activation of Erk pathways suppressed Schwann cell differentiation, whereas that of PI3K pathways promoted it. Furthermore, lithium chloride, a modulator of glycogen synthase kinase-3β (GSK-3β) promoted Schwann cell differentiation, suggesting the involvement of GSK-3β as a downstream molecule of PI3K–Akt pathways. Selective activation of PI3K pathways in Schwann cells by gene transfer also demonstrated increased myelination in *in vitro* Schwann cell–DRG neuron cocultures and *in vivo* allogenic nerve graft experiments. We conclude that signals mediated by PI3K–Akt are crucial for initiation of myelination and that the effects of growth factors are primarily dependent on the balance between Erk and PI3K–Akt activation. Our results also propose the possibility of augmenting Schwann cell functions by modulating intracellular signals in light of future cell therapies.

Key words: glia; intracellular; myelin; regeneration; transplantation; peripheral nerve

Introduction

Cell differentiation is delicately regulated by diverse extrinsic stimuli as well as by intrinsic programs in multiple tissues and organs (Jessen and Mirsky, 2002). In the light of recent attempts in cell therapies, artificial regulation of cell behaviors in a time-specific and space-specific manner is required (Casper et al., 2002). Therefore, a detailed investigation of cell differentiation is now a matter of great importance.

Schwann cells, myelin-forming cells in the PNS, arise from the neural crest and are called immature Schwann cells at embryonic day 16 (E16)–E17 in rats. They then lose the mitotic activity and form a 1:1 relationship with axons. At this stage, they are called promyelinating Schwann cells, expressing specific genes such as myelin-associated glycoprotein (MAG), Protein Zero (P0), and suppressed cAMP-inducible POU (SCIP) and reducing immature Schwann cell markers such as GFAP and neural cell adhesion molecule (Mirsky and Jessen, 2001). The evolution from imma-

ture Schwann cells to promyelinating Schwann cells is a critical step, because the earliest commitment toward myelin formation is believed to take place at this stage (Owens and Bunge, 1989; Arroyo et al., 1998).

Several growth factors, such as neuregulin, platelet-derived growth factor (PDGF) and insulin-like growth factor-I (IGF-I), play important roles in the differentiation of Schwann cells (Barres and Raff, 1999; Garbay et al., 2000). Their receptors are classified as receptor-type tyrosine kinases (RTKs), which transmit intracellular signals mainly through mitogen-activated protein kinase (MAPK) pathways and phosphatidylinositol-3-kinase (PI3K) pathways (Hunter, 1997). Classical MAPK pathways consist of the Ras–Raf–Mek (MAPK kinase)–Erk (extracellular signal-regulated kinase) signaling cascade; PI3K consists of two subunits, the adaptor subunit p85 and the catalytic subunit p110, and activates Akt, which in turn stimulates downstream molecules (Marshall, 1995; Yao and Cooper, 1995). Although these two pathways are activated by many growth factors, eventual cell behaviors vary depending on cell types and contexts (Rommel et al., 1999). However, little is known about how various ligands exhibit distinctive effects through these common intracellular pathways.

Neuregulin is expressed on the surface of axons, and various mutant mice studies have revealed that neuregulin is indispensable for expansion of the Schwann cell precursor pool (Lemke,

1996; Morris et al., 1999; Garratt et al., 2000). In the primary culture studies of immature Schwann cells, PDGF promotes proliferation but suppresses the expression of promyelinating markers. However, IGF-I promotes both proliferation and differentiation of Schwann cells (Davis and Stroobant, 1990; Stewart et al., 1996; Russell et al., 2000). Compared with many works related to ligands and their effects on cells, little is known about intracellular signals of Schwann cells. Therefore, our specific aim in this study was to elucidate the mechanism of intracellular signals from RTKs that control differentiation from immature Schwann cells to the promyelinating stage.

We investigated the signal transduction pathways of neuregulin, PDGF, and IGF-I in primary rat Schwann cells and found that Erk activation negatively regulated their level of differentiation, whereas activation of PI3K pathways promoted it. In addition, activating PI3K pathways in Schwann cells in *in vitro* coculture with dorsal root ganglion (DRG) neurons or in *in vivo* allogenic peripheral nerve graft studies could achieve increased myelin formation.

Materials and Methods

Reagents. Materials used for cell cultures included DMEM, DMEM–Ham's F12, poly-L-lysine hydrobromide, 5-fluoro-2-deoxyuridine, uridine, forskolin, AraC, nerve growth factor (NGF) 2.5S, fetal bovine serum (FBS), PDGF-BB, LiCl, 5-bromo-2-deoxyuridine (BrdU), and ascorbic acid (Sigma, St. Louis, MO), minimum essential medium and N2 supplement (Invitrogen, Rockville, MD), IGF-I (R&D, Minneapolis, MN), rh-HRG-β1 (neuregulin) [epidermal growth factor (EGF) domain] (Genzyme, Minneapolis, MN), and 2-(4-morpholinyl)-8-phenyl-1(4H)-benzopyran-4-one (LY294002; Cell Signaling, Beverly, MA). Monoclonal antibodies included anti-MBP (MAB382; Chemicon, Temecula, CA), anti-MEK1, anti-Erk, anti-Akt (Cell Signaling), anti-BrdU FITC-conjugated (Oxford Biotech, Oxford, UK), and anti-GSK-3 (Sigma). Rabbit polyclonal antibodies included anti-phospho-Akt (Ser 473), anti-phospho-Erk (Santa Cruz Biotechnology, Santa Cruz, CA), and anti-phospho-GSK-3 (Cell Signaling). Secondary antibodies included horseradish peroxidase-conjugated anti-mouse IgG and anti-rabbit IgG (Promega, Madison, WI) and Alexa-conjugated anti-mouse IgG (Molecular Probes, Eugene, OR). Other chemicals and reagents used in this study were of analytical grade.

Construction of adenovirus vectors. We used adenoviruses carrying constitutively active Mek1 (Ax-Mek^{CA}), dominant-negative Ras (Ax-Ras^{DN}), wild-type p110 (Ax-p110), myristoylated Akt (Ax-*myr*Akt), and dominant-negative p85 (Ax-p85^{DN}), all of which were generous gifts from H. Katagiri and T. Asano, The University of Tokyo, Tokyo, Japan (Katagiri et al., 1996, 1997; Mochizuki et al., 2002). Infection of the adenovirus vectors was performed as described in previous reports, and the effects of transgenes were assessed 48 hr after inoculation (Miura et al., 2000).

Cell cultures. Primary rat Schwann cells were isolated and cultured using the modified method of Brockes et al. (1979) (Mathon et al., 2001). Briefly, Schwann cells were taken from sciatic nerves of postnatal day 2 Wistar rats (Sankyo Labo Services, Tokyo, Japan) and cultured in DMEM containing 10% FBS. The next day, 10 μM AraC was added to the medium to eliminate contaminating fibroblasts. After 48 hr, the medium was replaced by DMEM containing 3% FBS with 3 μM forskolin and 20 ng/ml neuregulin to expand the cells. Cells were then detached from the dishes by 0.25% trypsin treatment and subcultured by replating at a 1:4 ratio onto poly-L-lysine-coated plastic dishes before confluence. We obtained a Schwann cell culture of >99% purity with these procedures. In all of the experiments, cells were used between passage 3 and 7. For adenovirus infection, cells were incubated with DMEM containing adenovirus vectors for 2 hr, and then the medium was changed to DMEM with 10% FBS and cultured for an additional 48 hr.

Reverse transcription-PCR of Schwann cell markers. Phenotypes of Schwann cells were assessed by reverse transcription (RT)-PCR. Cells were kept in DMEM with 10% FBS for 48 hr before each experiment, and

then indicated reagents were applied with fresh medium containing 3 μM forskolin. Total RNA was collected by an acid guanidinium thiocyanate–phenol-chloroform extraction procedure, using Isogen (Wako, Osaka, Japan) according to the manufacturer's protocols, and cDNA was obtained by Super Script II (Invitrogen, Carlsbad, CA) according to the manufacturer's protocol. PCR was performed using Super *Taq* (Sigma) with the following primers: MAG, 5′-ACTGGTGTGTAGCTGAGAAC-3′, 5′-GACAATGGCAATCAGGATGG-3′; P0, 5′-GCTCTTCTCTTCTTTGGT-GCTGTCC-3′, 5′-GGCGTCTGCCGCCCGCGCTTCG-3′; glyceraldehyde-3-phosphate dehydrogenase (GAPDH), 5′-GTATGTCGTGGAGTC-TACTGGCGT-3′, 5′-TACTCCTTGGAGGCCATGTAGGCC-3′; MBP (exon 3–5), 5′-ACTCACACACAAGAACTACCCA-3′, 5′-AGCTAAAT-CTGCTGAGGGACA-3′.

Real-time PCR was also performed using the TaqMan assay protocol of an ABI (Foster City, CA) Prism 7000 with the following: MAG primer, 5′-GGTACATGGCGTCTGGTATTTCA-3′ and 5′-CCACTTGTGTG-CGGGACTT-3′; probe, 5′-CAGTCCCTACCCCAAGAACTACCCGC-3′. The primer of rodent GAPDH was purchased from ABI.

Western blotting. Schwann cells were serum-starved with 0.1% FBS DMEM for 6 hr, and then the medium was changed to 0.1% FBS DMEM containing each growth factor at the indicated concentration. In cases in which adenovirus vectors were used, infection procedures were performed 2 d before the experiments. Fifteen minutes after growth factor stimulation, the cells were washed and lysed with lysis buffer (10 mM Tris-HCl, 1% NP-40, 0.1% sodium deoxycholate, 1 mM EDTA, 2 mM sodium orthovanadate, 10 mM sodium fluoride, and 10 μg/ml aprotinin). Samples containing an equal amount of protein (10 μg) were electrophoresed on SDS-polyacrylamide gels. Proteins were then transferred to Immobilon-P (Millipore, Bedford, MA). Primary antibodies were used in 1:1000 dilution at room temperature for 1 hr in 3% BSA TBS plus Tween 20 (TBST). The secondary antibodies were used in 1:10,000 dilution, and the immunoblots were developed by using the ECL system (Amersham Biosciences, Little Chalfont, UK).

Myelination assay. DRG neuron coculture with Schwann cells was performed using the modified method of Einheber et al. (1995). Briefly, DRGs were taken from E15 rats, dissociated with 0.25% trypsin, and seeded on 12 mm dishes coated with collagen type I at 200,000 cells per well. Non-neuronal cells were removed by treating cultures with C media (MEM, 10% FBS, 0.4% glucose, and 100 ng/ml 2.5S NGF) supplemented with 5-fluorodeoxyuridine, uridine, and AraC (at 10 μM) or with C media alone every 2–3 d alternately for 10 d. Schwann cells were cultured with C media without NGF for 2 d, infected with indicated adenoviruses for 2 hr, and inoculated in purified DRG neuron cultures at a density of 400,000 cells per well. The next day the medium was changed to DMEM–Ham's F12 with N2 supplement and NGF and kept for several days until axons were populated by Schwann cells. The medium was then replaced by C media with 50 ng/ml ascorbic acid to promote myelination. Cocultures were kept for 2 weeks and then fixed with 4% paraformaldehyde. Cells were permeabilized by treatment with 100% methanol at −20°C, and anti-MBP antibody diluted at 1:200 in TBST with 3% BSA was applied overnight at room temperature. Specimens were then washed, and secondary antibodies were added to observe myelin-forming Schwann cells by fluorescence microscopy. The number of myelin-forming Schwann cells was counted by surveying 20 fields at 200× magnification and expressed by percentage ratio to that in untreated control cultures. The average was calculated, and *p* values were obtained using Student's *t* test.

Sciatic nerve allogenic graft. To prepare graft segments, 10-week-old Wistar rats were anesthetized (50 mg/kg ketamine, 5 mg/kg xylazine), and the sciatic nerves were severed at the proximal site. The donor rats were kept alive for 2 weeks, at which time they were killed and the distal stump of the sciatic nerve was removed to make 8-mm-long grafts. The grafts were then incubated in DMEM with 10% FBS containing indicated adenoviruses for 4 hr before transplantation. The recipient 12-week-old Wistar rats were anesthetized, their sciatic nerves were exposed on one side, and 4 mm nerve segments were removed by sharp cut. Then *ex vivo* gene-transferred nerve segments were promptly placed to bridge the gaps and sutured with 10-0 nylon thread.

Histological analysis. The recipient rats were kept for 5 weeks, at which time the operated sciatic nerves were taken out after intracardial irriga-

tion with 4% paraformaldehyde. After fixation, the specimens were embedded in paraffin. For toluidine blue staining and electron microscopy, the specimens went through epon embedding. For immunostaining, paraffin-embedded samples were sectioned in the axial direction at 1 mm distal to the proximal end of the grafts and blocked with 3% BSA in TBST for 4 hr; anti-MBP antibody, diluted at 1:10, was then applied overnight at room temperature. Green fluorescent secondary antibody was used at a 1:100 dilution for 1 hr, and the samples were observed using a Carl Zeiss (Thornwood, NY) microscope. We studied 12 rats (6 Ax-LacZ and 6 Ax-*myr*Akt) and, to determine the extent of myelination, observed the entire area and calculated the number of myelinating nerve fibers per area. The data were analyzed by Mann–Whitney's *U* test.

BrdU labeling and detection. To determine the proliferation of the cells in the grafts, the recipient rats were injected on day 4 after implantation with BrdU (50 mg/kg, i.p.) every 3 hr for 24 hr; the rats then went through fixation 1 d after the final BrdU injection. The sections were denatured by reagents included in the BrdU detection kit (Zymed Laboratories, South San Francisco, CA) and stained with anti-BrdU FITC-conjugated monoclonal antibody. For survival assay of the implanted cells, the grafts were labeled with BrdU by oral administration (in 1 mg/ml drinking water) to the donor rats for 2 weeks. Specimens were taken 2 weeks after implantation and underwent the same procedures mentioned above.

Results

Modulation of Schwann cell differentiation by ligands of RTKs

MAG, P0, and MBP are myelin-related proteins, the expression of which was enhanced when primary rat Schwann cells were treated with forskolin (Fig. 1*A*). We assessed the effects of various growth factors on the expression of these molecules and found that their expression was suppressed by neuregulin and PDGF and increased by IGF-I (Fig. 1*A*). The quantification of MAG mRNA by real-time PCR showed an 80% reduction in MAG expression level with neuregulin (20 ng/ml) or PDGF (50 ng/ml) treatment but a 200% increase with IGF-I treatment (150 ng/ml) (Fig. 1*B*). We subsequently examined the intracellular signaling pathways underlying the effects of these growth factors. As shown in Figure 1*C* by Western blotting, neuregulin and PDGF strongly induced the phosphorylated form of Erk (i.e., Erk activation), whereas IGF-I had only limited potency in its activation. Quantification by densitometric analysis indicates that IGF-I phosphorylates Erk only 23% as much as does neuregulin. However, Akt activation was observed in the IGF-I-treated cells at a level comparable with that seen for the neuregulin-treated cells (Fig. 1*C*). Therefore, suppression of promyelinating markers seems to be related to the strong activation of Erk.

Suppression of Schwann cell differentiation by Erk pathways

To confirm the suppressive effect of Erk activation on MAG expression, we constructed adenovirus vectors to modulate these pathways. Infection with adenovirus vectors carrying dominant-negative *ras* gene (Ax-Ras[DN]) suppressed neuregulin-stimulated Erk phosphorylation but had minimal suppressive effects on phosphorylation of Akt (Fig. 2*A*). In contrast, constitutively active Mek virus (Ax-Mek[CA]) induced Erk phosphorylation in the absence of ligand stimulation (Fig. 2*C*). As shown in Figure 2*B* by RT-PCR, neuregulin treatment suppressed MAG expression induced by forskolin, and this suppressive effect was completely abrogated by Ras[DN] expression. However, Mek[CA]-expressing Schwann cells failed to respond to forskolin, and MAG expression was not observed (Fig. 2*D*). No significant change in MAG expression was observed in LacZ virus-infected cultures. These results clearly demonstrate the suppressive effect of Erk pathways on Schwann cell differentiation.
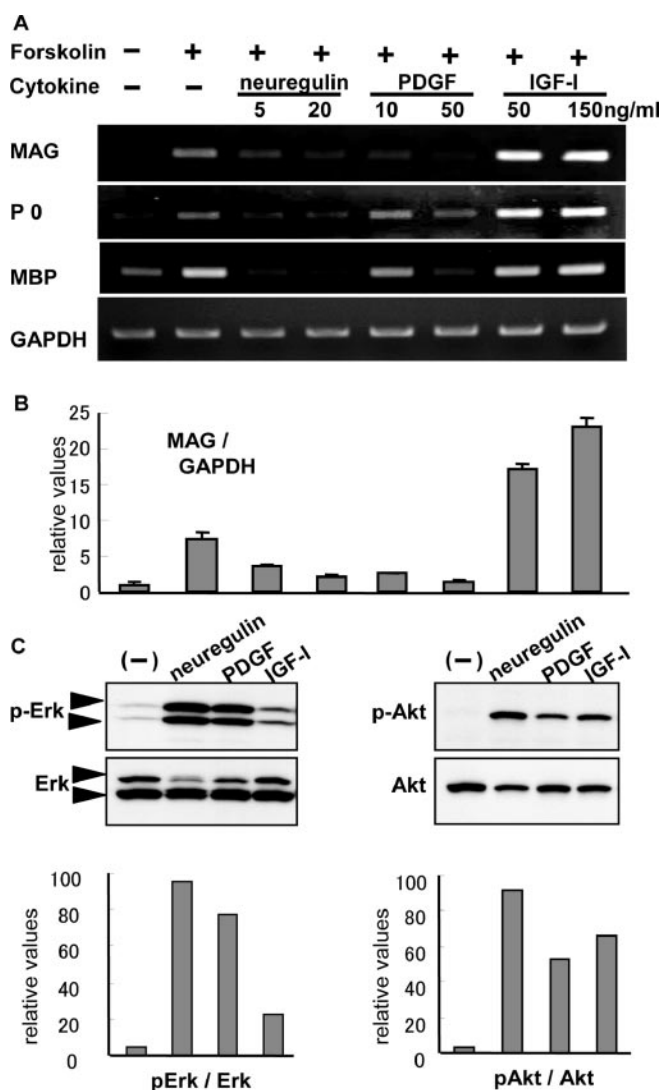

Figure 1. Regulation of MAG, P0, and MBP mRNA levels by various growth factors. *A, B,* Primary rat Schwann cells were exposed to various growth factors at the indicated concentration with or without forskolin, and the mRNA level of MAG, P0, MBP, and GAPDH was analyzed by RT-PCR (*A*) or real-time PCR (*B*) 24 hr later. Neuregulin and PDGF negatively regulate and IGF-I positively regulates MAG expression. *C,* The effect of neuregulin, PDGF, and IGF-I on the phosphorylation of Erk and Akt was examined by Western blot (top) and densitometric analysis (bottom). Robust phosphorylation of Erk was observed with neuregulin or PDGF treatment but not with IGF-I treatment. There were very minor differences in phosphorylation of Akt among the three growth factors. Concentrations were as follows: 3 μM forskolin, 20 ng/ml neuregulin, 50 ng/ml PDGF, and 150 ng/ml IGF-I if not indicated.

Essential role of PI3K–Akt pathways on MAG expression

We subsequently examined the role of PI3K pathways on MAG expression in Schwann cells using adenovirus vectors. We constructed adenovirus vectors carrying a dominant-negative mutant of the regulatory subunit p85 (Ax-p85[DN]), which negatively regulated PI3K pathways without influencing Erk pathways (Fig. 3*A*). The other vector, the catalytic subunit p110 (Ax-p110), positively regulated PI3K pathways, as shown in Figure 3*C* by Western blotting with anti-phosphorylated Akt antibody. RT-PCR analysis demonstrated that Schwann cells infected by Ax-p85[DN] did not respond to either forskolin alone or forskolin and IGF-I together, and the MAG mRNA was undetectable (Fig. 3*B*), indicating that PI3K pathways are necessary for MAG expression in the cells. Treating cells with LY294002 (40 μM), a specific inhib-
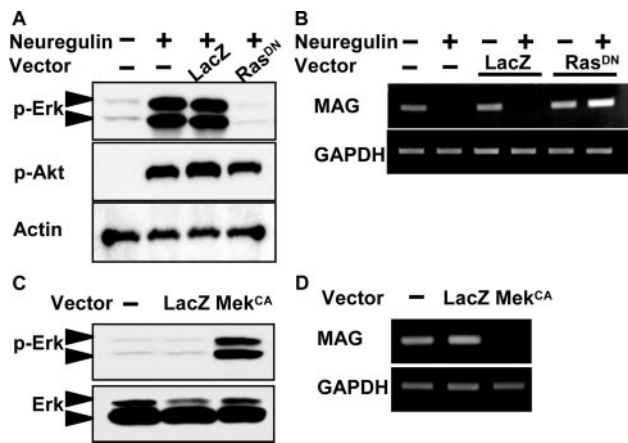
Figure 2. Erk has negative effects on MAG expression. *A*, Western blotting of anti-phospho-Erk antibody. Ax-Ras [DN] potently blocked the growth factor-induced Erk phosphorylation but exerted a slight suppressive effect on Akt phosphorylation. *B*, Effect of Ax-Ras [DN] on MAG expression was determined by RT-PCR. Note that the suppression of MAG mRNA by neuregulin was completely restored by Ax-Ras [DN]. *C, D,* Effect of Ax-Mek [CA] on MAG expression. MAG expression was completely abrogated by Ax-Mek [CA] (*D*), which induced strong Erk phosphorylation without ligand stimulation (*C*). Concentrations were as follows: 3 μM forskolin and 20 ng/ml neuregulin. Adenovirus vectors were used at a multiplicity of infection of 10.
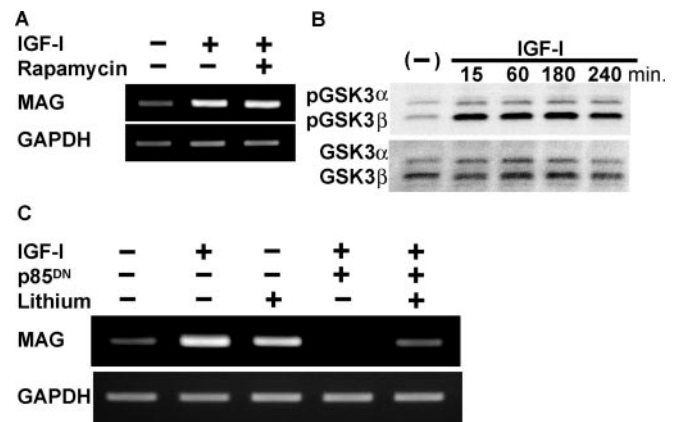

Figure 4. Involvement of GSK-3β downstream of Akt pathways. *A*, Effect of rapamycin on MAG expression in Schwann cells as determined by RT-PCR. Rapamycin did not affect MAG mRNA induced by IGF-I. *B*, Western blotting with anti-phospho-GSK-3β antibody. GSK-3β was phosphorylated in response to IGF-I stimulation in Schwann cells. *C*, Effect of LiCl on MAG expression in Schwann cells. Note the promoting effect of LiCl on MAG mRNA in the presence of forskolin. MAG mRNA was induced by forskolin and IGF-I but disappeared in the presence of Ax-p85 [DN]. The effect of LiCl was still observed even in the presence of Ax-p85 [DN], showing partial restoration of MAG expression. Concentrations were as follows: 16 mM LiCl, 1 μM rapamycin, and 3 μM forskolin.

To examine the downstream effectors of PI3K pathways, we used Ax-*myr*Akt, which contains an Src myristoylation signal that promotes association with the plasma membrane causing constitutive activation through phosphorylation by Akt-activating kinases. Similar to Ax-p110, Ax-*myr*Akt had positive effects on MAG expression (Fig. 3*E*), and quantification of MAG mRNA showed a twofold increase by Ax-*myr*Akt and a fourfold increase by Ax-p110 compared with the expression induced by forskolin alone (Fig. 3*E*). Because IGF-I activates PI3K–Akt pathways (Fig. 1*C*) and promotes MAG expression (Fig. 1*A*), these findings imply that IGF-I exerts its effects on MAG expression via PI3K–Akt pathways.

Possible participation of GSK-3β signaling in MAG expression
To further investigate the downstream signaling of Akt, we assessed the involvement of the mammalian target of rapamycin (mTOR) and GSK-3β, both of which are well known downstream molecules of PI3K–Akt pathways. Rapamycin is a specific inhibitor of mTOR pathways by forming an inhibitory complex with the immunophilin referred to as FK506 binding protein 12 (Hidalgo and Rowinsky, 2000). However, rapamycin did not affect MAG expression in Schwann cells, precluding a positive or negative effect of the pathways on Schwann cell differentiation (Fig. 4*A*). GSK-3β, the other target of Akt, transmits signals from various growth factors, including insulin, and regulates cell fates in development. The activity of GSK-3β is at least partly regulated by the phosphorylation and dephosphorylation of its N-terminal serine residue (serine-9), and GSK-3β usually suppresses the effector molecule when it is in a dephosphorylated state. When GSK-3β is phosphorylated by Akt, it becomes inactive, and its effector molecules become active (Cohen and Frame, 2001). As shown in Figure 4*B* by Western blotting, IGF-I treatment rapidly induced phosphorylation of GSK-3β without affecting its protein levels. LiCl is a well known inhibitor of GSK-3β activity, although its mechanism of action still remains elusive. LiCl was unable to induce MAG in Schwann cells when administered alone (data not shown); however, when LiCl was used at a concentration of 16
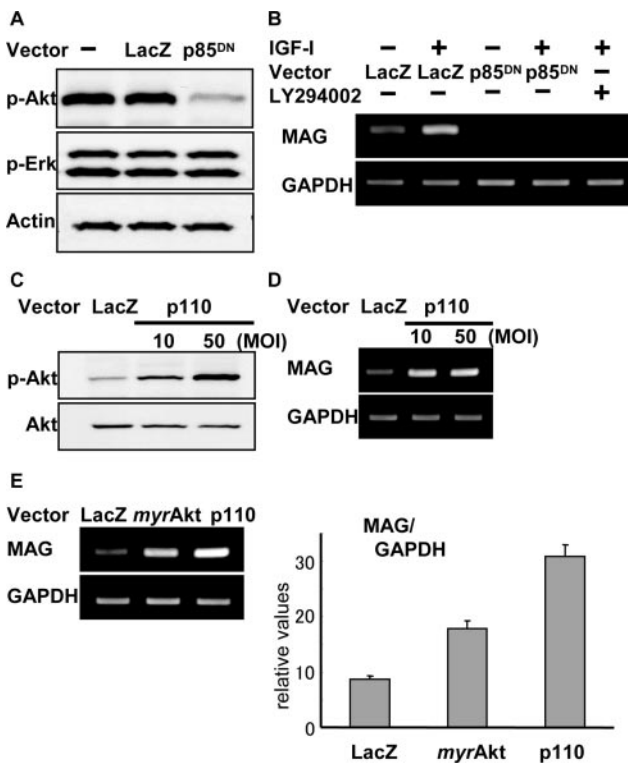

Figure 3. PI3K pathways are necessary for MAG expression. *A*, Ax-p85 [DN] diminished phosphorylation of Akt in response to growth factor stimulation. Phosphorylation of Erk was not altered by this vector. *B*, Ax-p85 [DN]-infected Schwann cells failed to express MAG mRNA in RT-PCR after induction by either forskolin alone or forskolin and IGF-I. *C, D,* Overexpression of p110 enhanced Akt phosphorylation (*C*) and enhanced MAG expression in the presence of forskolin (*D*). *E*, Ax-*myr*Akt enhanced MAG expression, and real-time PCR revealed a twofold increase by Ax-*myr*Akt and a fourfold increase by Ax-p110. MOI, Multiplicity of infection.

itor for PI3K, also markedly reduced MAG expression. In contrast, overexpression of p110 led to enhancement of MAG expression, suggesting that PI3K pathways are not only necessary for MAG expression but also promote its expression as induced by forskolin (Fig. 3*D*).

mM together with a 3 μM concentration of forskolin, it greatly enhanced forskolin-induced MAG expression (Fig. 4C). Over-expression of p85^{DN} strongly suppressed PI3K activity, and MAG was not detectable even in the presence of forskolin and IGF-I; however, MAG expression was partially restored when LiCl was applied to the medium (Fig. 4C). We assumed that LiCl at least partially compensated for the lack of PI3K activity by inactivating GSK-3β. These results imply that GSK-3β regulates some part of Schwann cell differentiation and is involved in IGF-I-mediated MAG upregulation.

Augmentation of myelin formation in Schwann cell–DRG neuron cocultures through PI3K–Akt pathways

To assess whether augmentation of MAG expression does in fact lead to myelin formation, we then performed coculture studies of Schwann cells with DRG neurons, a well established system to observe myelination *in vitro*. Schwann cells were infected by Ax-p110, Ax-*myr*Akt, Ax-p85^{DN}, or Ax-LacZ just before starting coculture and were added to purified DRG neuron cultures. With this method, we could exclusively modify intracellular signals of Schwann cells without affecting those of neurons. The medium was then changed to myelin-inducing medium containing ascorbate, and after 2 weeks of cocultures, cells were fixed and immunostained with anti-MBP antibody. The immunostaining demonstrated an increased number of myelin-forming cells in both the Ax-*myr*Akt-treated and Ax-p110-treated Schwann cell groups without affecting the total cell number (Fig. 5A). Figure 5B represents quantification of the results, which show a 1.5-fold increase in the Ax-*myr*Akt group and a threefold increase in the Ax-p110 group compared with the Ax-LacZ group, both of which are statistically significant. As for Ax-p85^{DN}, virtually no myelin formation was observed (Fig. 5A).

Enhanced myelination of regenerating axons in allogenic nerve graft via Ax-*myr*Akt

The clear potency of PI3K–Akt pathways on myelination led us to conduct *in vivo* experiments in which sciatic nerve segments of donor rats were gene-transferred *ex vivo* and grafted allogenically. Figure 6A schematically shows the procedure. The sciatic nerves of donor rats were severed at the proximal side. The nerve segments were taken out 2 weeks later, infected with adenovirus vectors for 4 hr *ex vivo*, and then transplanted into the freshly prepared sciatic nerve defects in recipient rats. The efficient gene transfer with adenovirus was confirmed by β-galactosidase staining of the Ax-LacZ group, shown in supplemental Figure 1, E and F (available at www.jneurosci.org/cgi/content/full/24/30/6724/DC1).

Five weeks after transplantation, specimens showed no myelin debris in either the Ax-*myr*Akt-infected or the Ax-LacZ-infected group, and the early stage of regenerating axons and myelination was observed
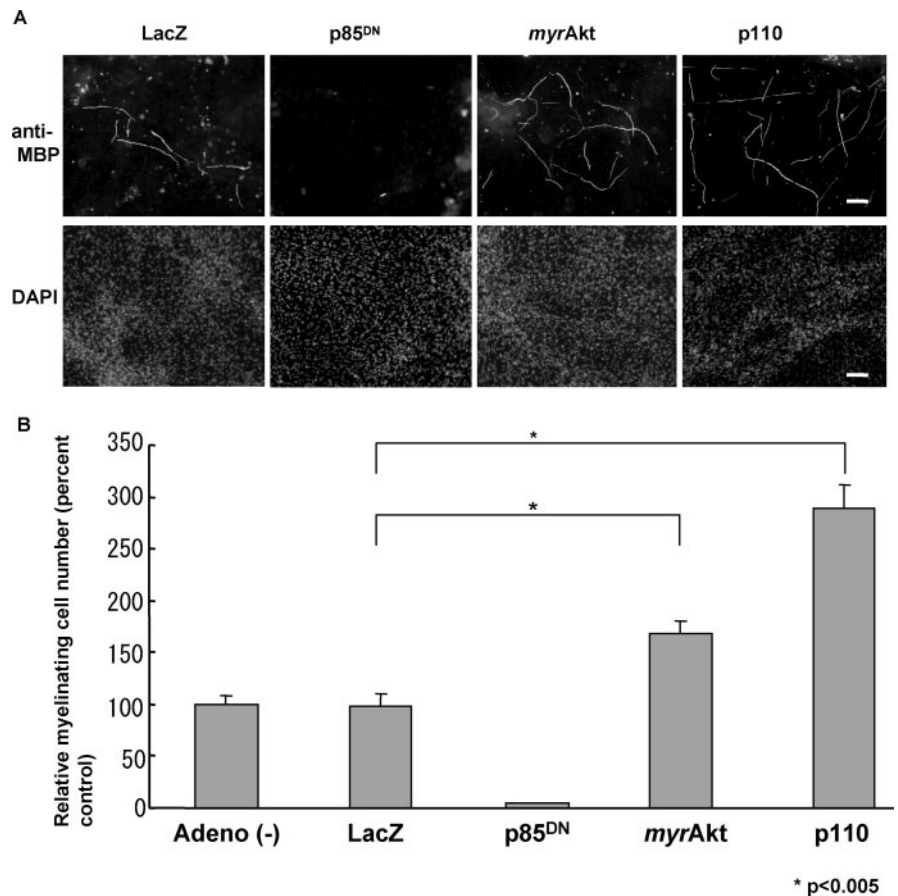

Figure 5. Ax-*myr*Akt-transferred Schwann cells formed more myelin in coculture with DRG neurons. *A*, DRG neurons were cocultured with gene-transferred Schwann cells using Ax-LacZ, Ax-p85^{DN}, Ax-*myr*Akt, or Ax-p110. Immunocytochemistry with anti-MBP antibody showed more myelin formation in Ax-*myr*Akt and Ax-p110 (top), whereas nuclear staining showed the same cell density in all groups (bottom). Virtually no myelin was observed in the Ax-p85^{DN}-transfected group. DAPI, 4′,6′-diamidino-2-phenylindole. *B*, The number of myelin-forming cells was counted, and a 1.5-fold increase in Ax-*myr*Akt and a threefold increase in Ax-p110 were observed. Scale bars, 50 μm.

(Fig. 6B,C). Electron microscopy revealed compartmental structures typically observed in regenerating peripheral nerves, and the myelinated fibers were observed more frequently in the Ax-*myr*Akt group than in the Ax-LacZ group, as shown in Figure 6, D and E. As for the thickness of each myelin sheath, we did not see a significant difference. Immunohistochemical analysis with anti-MBP antibody enabled us to quantify the degree of myelin formation. At the low-power view of Ax-LacZ-treated nerves, we found more myelin formation close to the perineurium and less at the center of the grafts in axial sections (Fig. 6F), whereas Ax-*myr*Akt-treated nerves showed evenly distributed myelinated axons (Fig. 6G). To evaluate myelin formation, we calculated the number of myelinated axons per area. Figure 6J shows 1.5-fold more myelin-forming axons in the Ax-*myr*Akt group with statistical significance. We also compared the proximal ends of the grafts and host nerves distal to the grafts and found that the difference between the Ax-myrAkt and Ax-LacZ groups was less obvious at the distal point (supplemental Fig. 2, available at www.jneurosci.org/cgi/content/full/24/30/6724/DC1).

To exclude any effects from transferred genes on cell functions other than differentiation, we assessed proliferation and survival of the cells in the grafts. On day 4 after transplantation, both the Ax-*myr*Akt and the Ax-LacZ group received repeated intraperitoneal BrdU injections to label proliferating cells at that time. We calculated the percentage of BrdU-positive cells among total cells. As shown in Figure 6K, there was no difference in proliferation between the two groups. We also assessed the survival ratio of the
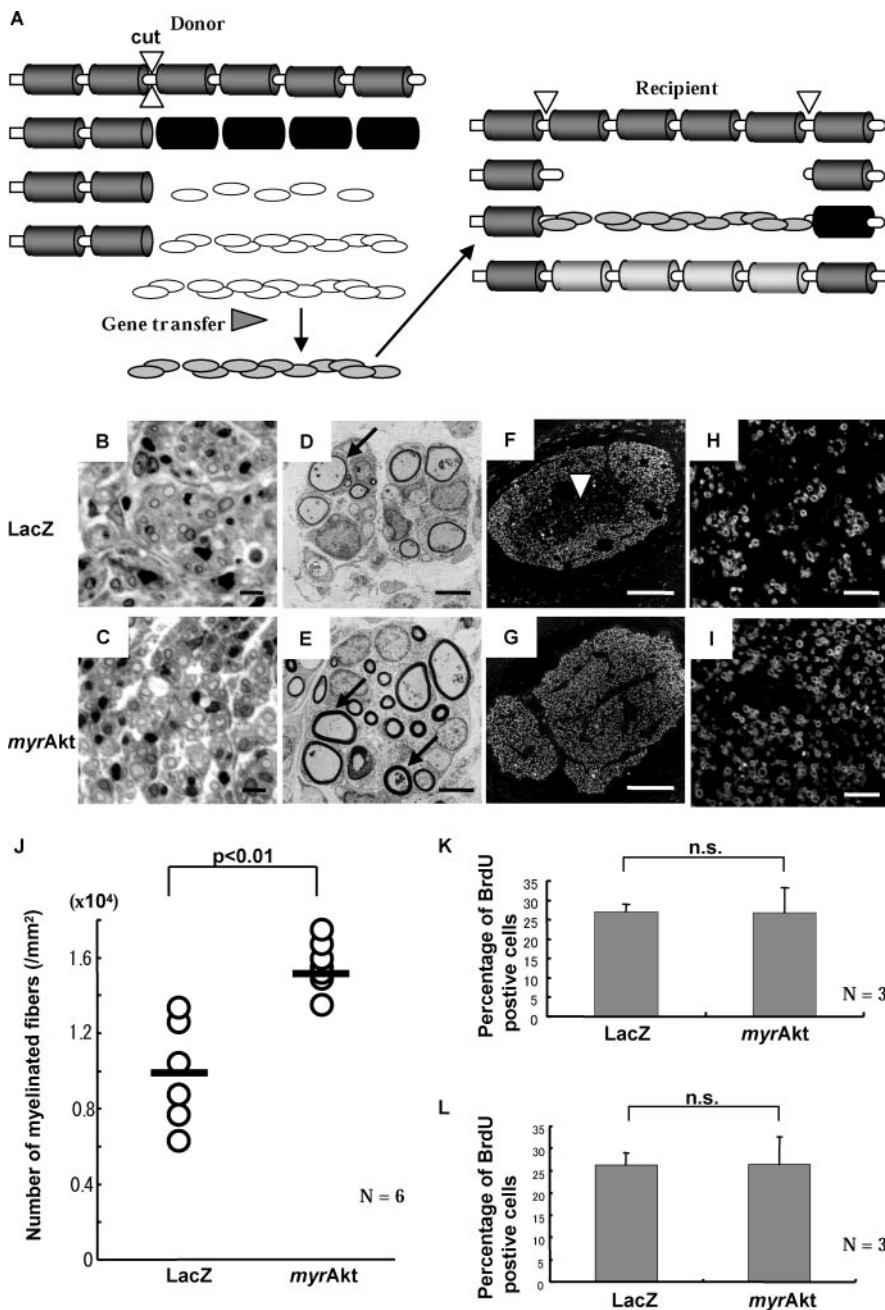
Figure 6. Histological analysis of *ex vivo* gene-transferred peripheral nerve grafting. *A*, Schematic procedures of allogenic nerve graft. *B–I*, Five week postoperative specimens of nerve graft infected either by Ax-LacZ (*B, D, F, H*) or Ax-*myr*Akt (*C, E, G, I*). Cross-sectional analysis by toluidine blue staining (*B, C*) and electron microscopy (*D, E*) indicated that regenerating fibers and the structures of myelin formation (*D, E*, arrows) were normal. Immunohistochemistry with anti-MBP antibody at low magnitude (*F, G*) showed that regenerating myelin fibers distribute sparsely near the center in Ax-LacZ group (arrowhead). *H, I*, A typical view near the center revealed more myelin formation in the Ax-*myr*Akt group. *J*, The number of myelinated fibers per area was calculated (6 rats per group). The average value (bar) shows increased myelination in the Ax-*myr*Akt group with statistical significance (*$p = 0.01$). *K*, Proliferating cells within implanted grafts were labeled by BrdU. The bars express the percentage of BrdU-positive cells among total cells, revealing that there was no difference between two groups ($n = 3$). *L*, The cells in the grafts were labeled before transplantation, and specimens were taken from the recipients 2 weeks after transplantation. Equivalent portions of cells were BrdU-positive between the two groups as shown in the graph ($n = 3$). n.s., Not significantly different. Scale bars: *B, C*, 10 μm; *D, E*, 5 μm; *F, G*, 200 μm; *H, I*, 50 μm.

cells within the grafts by labeling grafted cells with BrdU before transplantation. We took specimens from Ax-*myr*Akt-treated or Ax-LacZ-treated implants 2 weeks after the surgical procedures. Figure 6*L* shows the percentage of BrdU-positive cells among total cells in each group, which revealed that an equivalent amount of BrdU-positive cells was remaining in both groups. BrdU labeling also enabled us to confirm that BrdU-positive im-

planted cells colocalized with MBP and participated in remyelination (supplemental Fig. 3, available at www.jneurosci.org/cgi/content/full/24/30/6724/DC1).

Discussion

We observed different responses of Schwann cells to the three ligands of RTKs, neuregulin, PDGF, and IGF-I. Despite the important function of neuregulin in early Schwann cell development, it negatively regulates the expression of promyelinating Schwann cell markers. PDGF also had negative effects, whereas IGF-I exhibited positive effects. The similar divergent responses to growth factors have been described in other types of cells, such as pheochromocytoma 12 cells, a model for sympathetic neuronal differentiation, which extend neurites when they are treated by NGF but not by EGF (Marshall, 1995; Miura et al., 2000). The C2C12 myoblast cell line likewise forms myotubes in the presence of IGF-I, but fibroblast growth factor-2 (FGF-2) fails to induce differentiation (Tortorella et al., 2001).

It is now established that Ras–Raf–Mek–Erk and PI3K–Akt pathways are major downstream signaling pathways of RTKs. Although all three of the growth factors (neuregulin, PDGF, and IGF-I) activate these two pathways, the degree of activation differs, and the diverse level of activation of Erk pathways and PI3K pathways may explain the different effects of these growth factors on Schwann cell differentiation. Neuregulin and PDGF strongly activated Erk, whereas IGF-I was less potent in activating Erk pathways. However, IGF-I treatment induced Akt activation to a level comparable with neuregulin and PDGF. In the case of C2C12 cells, the level of Erk phosphorylation is higher in response to FGF-2 treatment than IGF-I (Tortorella et al., 2001), similar to our observation in Schwann cells. These results lead us to speculate that Erk pathways negatively regulate and PI3K–Akt pathways positively regulate MAG expression in Schwann cells and their differentiation. To further analyze the function of these signaling pathways, we used adenovirus vectors modulating downstream signaling of these growth factor receptors. The efficiency of gene transfer by adenoviral vectors was confirmed by LacZ or green fluorescent protein gene, as shown in supplemental Figure 1 (available at www.jneurosci.org/cgi/content/full/24/30/6724/DC1). Blocking the Erk pathway by Ras[DN] overexpression abrogated the inhibitory effect of neuregulin on MAG expression in primary rat Schwann cells, and selective activation of the pathway by Ax-Mek[CA] strongly suppressed MAG expression, clearly displaying the suppressive function of

Erk pathways on MAG expression. In contrast, PI3K pathways had stimulatory actions on MAG expression on the basis of the observation that (1) overexpression of p85[DN] or specific inhibitors of PI3K pathways suppressed MAG expression, and (2) overexpression of the catalytic subunit p110 or activated mutant of the downstream effector Akt (*myr*Akt) showed a stimulatory effect on MAG expression.

These results clearly show that PI3K pathways are potent in promoting Schwann cell differentiation; nonetheless, Ax-p110 alone failed to induce MAG in the absence of forskolin (data not shown), which is consistent with the observation that IGF-I requires cAMP signals to exert its differentiating effect on Schwann cells (Stewart et al., 1996). These results suggest the presence of cross-talk between these two pathways, and in fact, cAMP augments IGF-I-induced PI3K activities by enhancing phosphorylation of insulin receptor substrate 2 in FRTL-5 thyroid cells (Ariga et al., 2000). However, we failed to show the change in the phosphorylation state of Akt by forskolin treatment in Schwann cells (data not shown). Additional studies are required to explore the relationship of these pathways.

Although MAG expression in Schwann cells was strongly suppressed by PI3K inhibitors, it was not affected by the mTOR inhibitor rapamycin. In contrast, LiCl, which is known to inactivate GSK-3β, promoted MAG expression in the presence of forskolin. These results suggest that GSK-3β, but not mTOR, is a downstream effector of PI3K–Akt pathways in Schwann cell differentiation. The inability of LiCl to induce MAG by itself further supports our findings that PI3K pathways require cAMP signals to exert their functions. Collectively, we presume that IGF-I conveys its signal through PI3K–Akt–GSK-3β pathways to promote MAG expression in the presence of forskolin. In addition to phosphorylating glycogen synthase, GSK-3β is reported to regulate the transcriptional activities of cAMP response element-binding protein and activator protein-1 or the stability of cyclin D1 and c-*myc* (Cohen and Frame, 2001; Grimes and Jope, 2001). Therefore, it is possible that cAMP and GSK-3β coordinately regulate gene expression and the activity of transcriptional factors binding to the MAG promoter region. It should be noted that LiCl exerted only partial recovery of Ax-p85[DN]-induced suppression of MAG expression, suggesting that some other molecules might be involved downstream of PI3K pathways.

The results of coculture experiments confirmed that the augmentation of PI3K pathways in Schwann cells not only increases MAG expression but also promotes myelin formation. Although the importance of PI3K has been suggested from coculture studies using LY294002 (Maurel and Salzer, 2000), our design of coculture enables us to modulate Schwann cells specifically and permits the more precise understanding of the signal transduction pathways regulating myelination. Several studies used a similar approach, using PKA inhibitory retroviral vectors or mutated IκB adenoviruses to inhibit nuclear factor κB, and they reported reduced myelination in cocultures as the result of interference in these pathways (Howe and McCarthy, 2000; Nickols et al., 2003). Recently, activation of p38 was also reported to be necessary for myelin formation (Fragoso et al., 2003). Our results imply not only the necessity of PI3K signals in myelination together with these signal pathways but also the potential of augmenting PI3K pathways to further increase myelin formation. We also used Ax-Mek[CA] in the coculture experiment. After several days from starting coculture, however, the Schwann cells treated with Ax-Mek[CA] took spherical forms rather than ensheathing axons. Finally, there was no myelin formation in the Ax-Mek[CA]-treated group (data not shown). Together with previous reports of the

suppressive effects of neuregulin on myelin formation in coculture (Zanazzi et al., 2001), we assume that the Schwann cell differentiation is accompanied by the negative regulation of Mek–Erk pathways.

In the transplantation experiments, we chose preconditioned sciatic nerves as grafts and *ex vivo* gene transfer before implantation. This gene transfer method enables us to modulate cells in the grafts exclusively without affecting the tissues or cells of the recipient side. We can therefore attribute the difference to the altered function of grafted cells. As for the reason we chose preconditioned nerves, we observed that the efficiency of adenovirus infection was much better in preconditioned nerves than in fresh nerves (data not shown).

To exclude various effects delivered by transferred genes, we performed BrdU labeling and confirmed that cell behaviors in terms of proliferation and survival after grafting were similar between the Ax-*myr*Akt and Ax-LacZ groups. With regard to the features of myelin immunostaining, the difference between Ax-*myr*Akt and Ax-LacZ groups was prominent in the central area of the grafts in axial sections. Significantly more fibers with myelin sheath were observed in Ax-*myr*Akt-infected grafts compared with the sparse distribution of the myelinated fibers in Ax-LacZ-infected grafts. This difference was only observed within the grafts but not at distal points in host nerves, implying that cells in the transplanted grafts caused the difference. The difference in myelin formation number in the central area of the grafts suggests that Ax-*myr*Akt promotes the differentiation of Schwann cells located
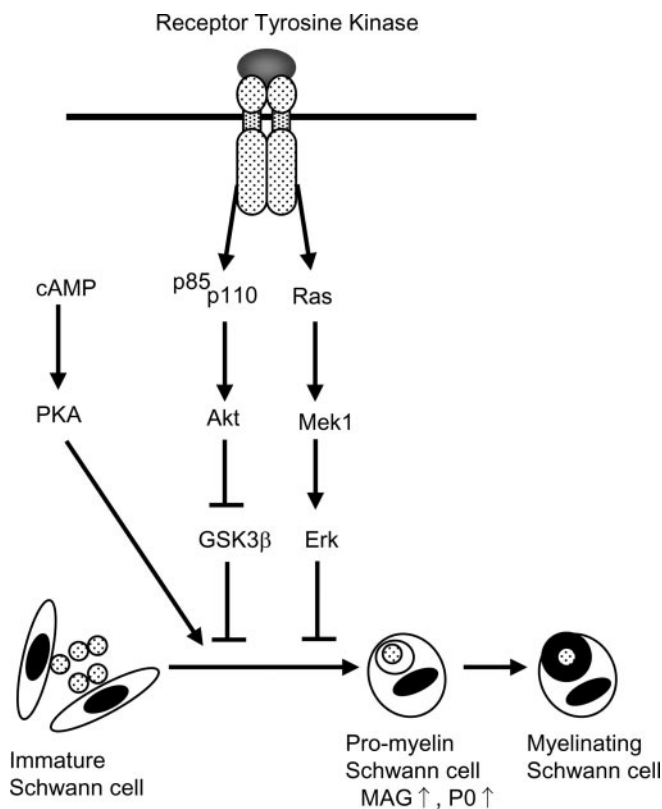

Figure 7. Schematic view of intracellular signaling cascades triggered by receptor tyrosine kinase in Schwann cells. We propose that upregulation of MAG mRNA implies a transition from immature Schwann cell to the promyelinating state and that myelination will subsequently occur. Activation of both cAMP and Akt–GSK-3β signals and, at the same time, downregulation of MAPK are all required for MAG expression. At present, the targets of these three pathways are not known.

in an unfavorable environment for myelin formation (Akassoglou et al., 2002). Collectively, our results from *in vivo* experiments suggest the importance of PI3K–Akt signals in myelination not only *in vitro* but also *in vivo*.

Although the physiological roles of Akt pathways in the development and the regeneration of the peripheral nervous system are still unknown, several reports have proposed the importance of IGF-I in myelin formation *in vivo*. Increased myelination was observed in IGF-I transgenic mice (Ye et al., 1995), whereas IGF-I-deficient mice showed impaired myelination in early development (Ye et al., 2002). Peripheral nerve grafting was also performed with local administration of IGF-I, and enhanced maturation of grafted nerves was reported (Fansa et al., 2002). Our results shed light on the mechanisms of these effects of IGF-I and reveal that IGF-I activates Akt pathways in Schwann cells and promotes differentiation. Because we could not fully exclude the participation of survival effects of Akt pathways in our experiment (Cheng et al., 2000), further understanding of Schwann cell differentiation will require separate modifications of survival and differentiation signals.

Schwann cells are now regarded as a possible candidate for various cell therapies or gene therapies, such as artificial nerves containing Schwann cells (Cheng and Chen, 2002) or transplantational therapy for demyelinating disorders, multiple sclerosis (Halfpenny et al., 2002), or traumatic lesions of the CNS such as spinal cord injury (Bunge, 2002). So far, the behavior of the cells after transplantation is uncontrollable, and little has been revealed about what factors affect the behavior of the cells and through what mechanisms. To put such therapies into practice, it is necessary to elicit intracellular mechanisms of Schwann cell differentiation and identify the target of therapeutic modification. We propose that PI3K–Akt–GSK-3β pathways mediate Schwann cell transition from the immature to promyelinating stage and are a crucial step in myelin formation (schematically shown in Fig. 7). The augmentation of these pathways can be a novel therapeutic approach to various disorders by effectively enhancing myelin formation.

References

Akassoglou K, Yu WM, Akpinar P, Strickland S (2002) Fibrin inhibits peripheral nerve remyelination by regulating Schwann cell differentiation. Neuron 33:861–875.

Ariga M, Nedachi T, Akahori M, Sakamoto H, Ito Y, Hakuno F, Takahashi S (2000) Signalling pathways of insulin-like growth factor-I that are augmented by cAMP in FRTL-5 cells. Biochem J 348:409–416.

Arroyo EJ, Bermingham Jr JR, Rosenfeld MG, Scherer SS (1998) Promyelinating Schwann cells express Tst-1/SCIP/Oct-6. J Neurosci 18:7891–7902.

Barres BA, Raff MC (1999) Axonal control of oligodendrocyte development. J Cell Biol 147:1123–1128.

Brockes JP, Fields KL, Raff MC (1979) Studies on cultured rat Schwann cells. I. Establishment of purified populations from cultures of peripheral nerve. Brain Res 165:105–118.

Bunge MB (2002) Bridging the transected or contused adult rat spinal cord with Schwann cell and olfactory ensheathing glia transplants. Prog Brain Res 137:275–282.

Casper D, Engstrom SJ, Mirchandani GR, Pidel A, Palencia D, Cho PH, Brownlee M, Edelstein D, Federoff HJ, Sonstein WJ (2002) Enhanced vascularization and survival of neural transplants with ex vivo angiogenic gene transfer. Cell Transplant 11:331–349.

Cheng B, Chen Z (2002) Fabricating autologous tissue to engineer artificial nerve. Microsurgery 22:133–137.

Cheng HL, Steinway M, Delaney CL, Franke TF, Feldman EL (2000) IGF-I promotes Schwann cell motility and survival via activation of Akt. Mol Cell Endocrinol 170:211–215.

Cohen P, Frame S (2001) The renaissance of GSK3. Nat Rev Mol Cell Biol 2:769–776.

Davis JB, Stroobant P (1990) Platelet-derived growth factors and fibroblast growth factors are mitogens for rat Schwann cells. J Cell Biol 110:1353–1360.

Einheber S, Hannocks MJ, Metz CN, Rifkin DB, Salzer JL (1995) Transforming growth factor-beta 1 regulates axon/Schwann cell interactions. J Cell Biol 129:443–458.

Fansa H, Schneider W, Wolf G, Keilhoff G (2002) Influence of insulin-like growth factor-I (IGF-I) on nerve autografts and tissue-engineered nerve grafts. Muscle Nerve 26:87–93.

Fragoso G, Robertson J, Athlan E, Tam E, Almazan G, Mushynski WE (2003) Inhibition of p38 mitogen-activated protein kinase interferes with cell shape changes and gene expression associated with Schwann cell myelination. Exp Neurol 183:34–46.

Garbay B, Heape AM, Sargueil F, Cassagne C (2000) Myelin synthesis in the peripheral nervous system. Prog Neurobiol 61:267–304.

Garratt AN, Voiculescu O, Topilko P, Charnay P, Birchmeier C (2000) A dual role of erbB2 in myelination and in expansion of the Schwann cell precursor pool. J Cell Biol 148:1035–1046.

Grimes CA, Jope RS (2001) CREB DNA binding activity is inhibited by glycogen synthase kinase-3 beta and facilitated by lithium. J Neurochem 78:1219–1232.

Halfpenny C, Benn T, Scolding N (2002) Cell transplantation, myelin repair, and multiple sclerosis. Lancet Neurol 1:31–40.

Hidalgo M, Rowinsky EK (2000) The rapamycin-sensitive signal transduction pathway as a target for cancer therapy. Oncogene 19:6680–6686.

Howe DG, McCarthy KD (2000) Retroviral inhibition of cAMP-dependent protein kinase inhibits myelination but not Schwann cell mitosis stimulated by interaction with neurons. J Neurosci 20:3513–3521.

Hunter T (1997) Oncoprotein networks. Cell 88:333–346.

Jessen KR, Mirsky R (2002) Signals that determine Schwann cell identity. J Anat 200:367–376.

Katagiri H, Asano T, Ishihara H, Inukai K, Shibasaki Y, Kikuchi M, Yazaki Y, Oka Y (1996) Overexpression of catalytic subunit p110alpha of phosphatidylinositol 3-kinase increases glucose transport activity with translocation of glucose transporters in 3T3–L1 adipocytes. J Biol Chem 271:16987–16990.

Katagiri H, Asano T, Inukai K, Ogihara T, Ishihara H, Shibasaki Y, Murata T, Terasaki J, Kikuchi M, Yazaki Y, Oka Y (1997) Roles of PI 3-kinase and Ras on insulin-stimulated glucose transport in 3T3–L1 adipocytes. Am J Physiol 272:E326–E331.

Lemke G (1996) Neuregulins in development. Mol Cell Neurosci 7:247–262.

Marshall CJ (1995) Specificity of receptor tyrosine kinase signaling: transient versus sustained extracellular signal-regulated kinase activation. Cell 80:179–185.

Mathon NF, Malcolm DS, Harrisingh MC, Cheng L, Lloyd AC (2001) Lack of replicative senescence in normal rodent glia. Science 291:872–875.

Maurel P, Salzer JL (2000) Axonal regulation of Schwann cell proliferation and survival and the initial events of myelination requires PI 3-kinase activity. J Neurosci 20:4635–4645.

Mirsky R, Jessen KR (2001) Embryonic and early postnatal development of Schwann cells. In: Glial cell development, Ed 2 (Jessen KR, Richardson WD, eds), pp 1–20. New York: Oxford UP.

Miura T, Tanaka S, Seichi A, Arai M, Goto T, Katagiri H, Asano T, Oda H, Nakamura K (2000) Partial functional recovery of paraplegic rat by adenovirus-mediated gene delivery of constitutively active MEK1. Exp Neurol 166:115–126.

Mochizuki T, Asai A, Saito N, Tanaka S, Katagiri H, Asano T, Nakane M, Tamura A, Kuchino Y, Kitanaka C, Kirino T (2002) Akt protein kinase inhibits non-apoptotic programmed cell death induced by ceramide. J Biol Chem 277:2790–2797.

Morris JK, Lin W, Hauser C, Marchuk Y, Getman D, Lee KF (1999) Rescue of the cardiac defect in ErbB2 mutant mice reveals essential roles of ErbB2 in peripheral nervous system development. Neuron 23:273–283.

Nickols JC, Valentine W, Kanwal S, Carter BD (2003) Activation of the transcription factor NF-kappaB in Schwann cells is required for peripheral myelin formation. Nat Neurosci 6:161–167.

Owens GC, Bunge RP (1989) Evidence for an early role for myelin-associated glycoprotein in the process of myelination. Glia 2:119–128.

Rommel C, Clarke BA, Zimmermann S, Nunez L, Rossman R, Reid K, Moel-

ling K, Yancopoulos GD, Glass DJ (1999) Differentiation stage-specific inhibition of the Raf-MEK-ERK pathway by Akt. Science 286:1738–1741.

Russell JW, Cheng HL, Golovoy D (2000) Insulin-like growth factor-I promotes myelination of peripheral sensory axons. J Neuropathol Exp Neurol 59:575–584.

Stewart HJ, Bradke F, Tabernero A, Morrell D, Jessen KR, Mirsky R (1996) Regulation of rat Schwann cell Po expression and DNA synthesis by insulin-like growth factors in vitro. Eur J Neurosci 8:553–564.

Tortorella LL., Milasincic DJ, Pilch PF (2001) Critical proliferation-independent window for basic fibroblast growth factor repression of myogenesis via the p42/p44 MAPK signaling pathway. J Biol Chem 276:13709–13717.

Yao R, Cooper GM (1995) Requirement for phosphatidylinositol-3 kinase in the prevention of apoptosis by nerve growth factor. Science 267:2003–2006.

Ye P, Carson J, D'Ercole AJ (1995) *In vivo* actions of insulin-like growth factor-I (IGF-I) on brain myelination: studies of IGF-I and IGF binding protein-1 (IGFBP-1) transgenic mice. J Neurosci 15:7344–7356.

Ye P, Li L, Richards RG, DiAugustine RP, D'Ercole AJ (2002) Myelination is altered in insulin-like growth factor-I null mutant mice. J Neurosci 22:6041–6051.

Zanazzi G, Einheber S, Westreich R, Hannocks MJ, Bedell-Hogan D, Marchionni MA, Salzer JL (2001) Glial growth factor/neuregulin inhibits Schwann cell myelination and induces demyelination. J Cell Biol 152:1289–1299.